Detection of silver nanoparticles in seawater at ppb levels using UV-Visible spectrophotometry with long path cells

Pablo Lodeiro[a,1*], *Eric P. Achterberg*[a,1] *and Mohammad S. El-Shahawi*[b,2]

[a]*Ocean and Earth Science, University of Southampton, National Oceanography Centre, European Way, SO14 3ZH Southampton, UK.*

[b]*Department of Chemistry, Faculty of Science, Damietta University, Damietta, Egypt.*

**Corresponding Author: plodeiro@geomar.de*

Present Addresses:

[1]GEOMAR, Helmholtz Centre for Ocean Research Kiel, Wischhofstraße 1-3, 24148 Kiel, Germany.

[2]*Department of Chemistry, Faculty of Science, King Abdulaziz University, P. O. Box 80203, Jeddah 21589, Kingdom of Saudi Arabia (on sabbatical leave)*

Abstract

Silver nanoparticles (AgNPs) are emerging contaminants that are difficult to detect in natural waters. UV-Visible spectrophotometry is a simple technique that allows detection of AgNPs through analysis of their characteristic surface plasmon resonance band. The detection limit for nanoparticles using up to 10 cm path length cuvettes with UV-Visible spectrophotometry is in the 0.1 to 10 ppm range. This detection limit is insufficiently low to observe AgNPs in natural environments. Here we show how the use of capillary cells with an optical path length up to 200 cm, forms an excellent technique for rapid detection and quantification of non-aggregated AgNPs at ppb concentrations in complex natural matrices such as seawater.

Keywords: Silver nanoparticles; seawater; NM300K; surface plasmon resonance band; UV-Visible spectrophotometry; long path cell.

Introduction

The increasing use of silver nanoparticles (AgNPs) in consumer products is raising concerns about their behaviour, fate and toxicological effects following discharge into natural waters [1]. The transformations of AgNPs through aggregation and oxidation processes, and their interactions in the environment, make their detection and quantification challenging. Furthermore, their low environmental concentrations, typically in the ppt range, forms a major analytical detection problem for the most commonly used analytical techniques, which include Light Scattering and UV-Visible spectrophotometry.

Based on the projected increase in AgNP production and release, the environmental concentrations of AgNPs in river waters by the year 2020 is projected to range between 225 and 1799 ppt total Ag [2]. Currently, the use of mass spectrometric techniques (e.g. ICP-MS, single particle ICP-MS) together with hyphenated systems such as asymmetric flow field-flow fractionation, capillary electrophoresis or liquid chromatography, allows for AgNP quantification in environmental samples at ppt-ppb levels [3-5]. The equipment is however complex and expensive with high running costs, and hence not available in most laboratories. Moreover, the sample analysis is destructive, requires multiple steps, long sample preparation times and well-trained operators.

UV-Visible spectrophotometry is a readily accessible technique that has been widely used to identify, characterize and study the stability of metallic NPs at elemental concentrations in the 0.1 to 10 ppm range [6, 7]. The surface plasmon resonance band (SPRB) of Ag, Au and Cu NPs is used in these studies, being the result of collective oscillations of the conduction electrons in resonance with the incident light frequency. Therefore, changes to the surface plasmon properties have been extensively utilised to determine NP aggregation processes in different media due to the high sensitivity of SPRB to NP size, shape and chemical composition [8-10].

76 UV-Visible spectrophotometry allows rapid and high-resolution detection (full spectra within
77 <1s using array-based spectrometers), on-site measurements, and is applicable to complex
78 matrices such as seawater. However, applications have been hampered due to the relatively
79 high detection limit (sub-ppm) for NPs, with the use of 1 or 10 cm path length cuvettes. The
80 absorbance of the analyte (A) is proportional to the optical path length (l), so a decrease in
81 the detection limit is obtained with increasing the cuvette length. In the present work, we
82 report the use of long path cells (100 to 200 cm) in UV-Visible spectrophotometry to enhance
83 the precision and accuracy, and decrease the detection limit for metallic NPs by at least one
84 order of magnitude. Knowledge of the molar attenuation coefficient (ε) of the NP under study
85 in the sample matrix is required to obtain NP concentrations from absorbance measurements
86 [11]. Limited information is available on this parameter for specific NPs, so we have
87 determined it for a reference AgNP material NM300K using a calibration in high-purity
88 water. The obtained molar attenuation coefficient was later used to quantify the presence of
89 non-aggregated AgNPs, previously spiked in two different natural seawaters.
90

91 **Materials and methods**

92 A silver reference nanomaterial (NM300K) from the Fraunhofer Institute for Molecular
93 Biology and Applied Ecology was used. The reference material consists of colloidal silver
94 spherical nanoparticles with a particle size ~15 nm (90% < 20 nm). The stabilizing capping
95 agent is an aqueous mixture comprising 4% (w/w) polyoxyethylene glycerol trioleate and 4%
96 (w/w) polyoxyethylene sorbitan monolaurate (Tween-20).
97 The laboratory chemicals used were purchased from Sigma-Aldrich (Dorset, UK) and Fisher
98 Scientific (Leicestershire, UK). We made use of high-purity water (MilliQ, Millipore,
99 Watford, UK) with a resistivity of >18.2 MΩ cm^{-1}. The natural surface water samples were
100 collected in a Baltic fjord located in northwest Germany (54°22.1' N 10º11.7' E) and A

101 Coruña Bay (43º21.8' N 8º23.4' W) in northwest Spain. The samples were stored in acid-
102 cleaned low-density polyethylene bottles (Nalgene) until use.
103 The UV-Visible spectra were recorded using a deuterium-halogen light source (DH2000,
104 Ocean Optics), two liquid waveguide capillary cells of 100 and 200 cm path length (LWCC,
105 World Precision Instruments) and a miniature CCD array spectrophotometer (USB-4000,
106 Ocean Optics), connected through two optical fibres (600 μm fibre, P600-025-SR). Using this
107 set-up and an in-house Matlab script we obtained a complete scan from 300 to 650 nm in <1
108 s. Solutions without AgNPs were used to blank correct the instrument. The solutions were
109 pumped through the capillary cell using a peristaltic pump (Watson-Marlow 400B series) in a
110 recirculation mode at constant flow rate (1.5 mL min^{-1}). The observed absorbance includes
111 surface plasmon resonance band (SPRB) effects and also scattering by disperse NPs,
112 especially at large sizes.
113 The total Ag content was measured by ICP-MS (Quadrupole Thermo X-Series 2) after
114 dilution and digestion of the samples with 0.3 M HNO_3 (70% Optima, Fisher Scientific). The
115 total Ag concentration measured in the NM300K AgNP solution was 102 ± 1 ppm. This
116 solution was tenfold diluted to obtain our stock AgNP NM300K solution.
117 The NM300K AgNP solutions (20 to 92 ppb) were prepared for the calibrations by addition
118 of increasing amounts of the stock solution (30, 60, 85, 115 and 135 μL) to high-purity water
119 (15 mL) at pH 8.0 ± 0.2 fixed using NaOH.
120 The obtained data was analysed in terms of SPRB evolution (maximum height, area, width at
121 half peak height and position of the absorbance maximum) over time. The SPRB values were
122 determined for at least two independent experiments, as an average of NM300K SPRB
123 evolution with time, after 10 minutes of mixing. The uncertainties in the SPRB measurements
124 were obtained as standard deviation of the different SPRB height values obtained.
125

126 **Results and discussion**

127 The measurement of the AgNP concentration in solution using UV-Visible
128 spectrophotometry requires the determination of its attenuation coefficient. The AgNP
129 NM300K attenuation coefficient was obtained through calibration using the Lambert-Beer
130 equation ($A= \varepsilon \cdot l \cdot c$). The AgNPs NM300K form a monodisperse suspension in high-purity
131 water. Therefore, we consider that the absorbance is proportional to the height of the SPRB.
132 Figure 1 shows the plot of the height of the SPRB *vs* AgNP concentration (c). The calibration
133 showed a linear relationship with good correlation coefficients.
134 The molar attenuation coefficient was determined from the slope of the calibration graph
135 using a 100 cm optical path length cell. High quality molar attenuation coefficients
136 determination requires a stable and low noise signal. We obtained an improved signal using a
137 100 cm cell because the optical transmission is between 36-40% higher in the 325-500 nm
138 range compared with a 200 cm length cell. The obtained value was $\varepsilon= 1.14\times10^{9}$ $M^{-1}cm^{-1}$.
139 Based on theoretical Mie calculations, the molar attenuation coefficient for idealised AgNPs
140 should be 2.8×10^{9} $M^{-1}cm^{-1}$ [12]. This value is more than twofold our experimental value, but
141 it is in close agreement with an experimentally obtained ε value for a 15 nm citrate-capped
142 AgNP (between $1.58\text{-}2.27\times10^{9}$ $M^{-1}cm^{-1}$) [11]. The observed minor discrepancies are
143 explained by the differences in AgNP coatings that result in modifications of their optical
144 properties [13].
145 Variations in SPRB height during the calibration experiment were investigated. The height of
146 the SPRB obtained in stable aqueous solutions of AgNPs slowly diminished over time with a
147 decrease in the total Ag concentration. At the lowest Ag concentration (20 ppb), the decrease
148 in SPRB height was ca. 8% over a period between 10 and 90 min. This observation was
149 attributed to slow dissolution kinetics of the AgNPs to Ag ions that occur at very low NP
150 concentrations due to light absorption and a temperature increase inside the capillary cell

151 produced by the light beam. Nevertheless, at Ag concentrations higher than 41 ppb,
152 variations of the SPRB height over 10 to 90 min were only between 0.5-1%. Moreover, the
153 position of the SPRB during the calibration measurements in high-purity water was stable at
154 413-416 nm, with a width at half height around 72-75 nm (76-80 nm for the highest tested
155 concentration of 92 ppb).
156 The main aim of our work was to quantify the change in NM300K AgNP concentrations
157 during their aggregation/dissolution in seawaters with different dissolved organic carbon
158 (DOC) contents and salinities. To achieve that objective we used the molar attenuation
159 coefficient obtained from the calibration. This allowed us for rapid detection and
160 quantification of non-aggregated AgNPs in different complex matrices. A 200 cm instead of
161 the 100 cm length cell was used when measuring the AgNP concentration in seawater with
162 UV-Visible spectrophotometry. The 100 cm cell provided a lower noise in the measured
163 signal, but doubling the path length a twofold lower NP detection limit was obtained. We
164 confirmed this approach through analyses of the peak height of the SPRB obtained upon
165 addition of stock solution with a final AgNP concentration of 20 ppb. Therefore, we
166 calculated the AgNP concentration in high-purity water when using 200 cm cells using the
167 obtained ε value. Table 1 shows that the concentration value was in good agreement with the
168 one calculated from the calibration.
169 The SPRB evolution over time following NM300K AgNP additions (initial concentration 20
170 ppb) was monitored here for the first time by UV-Visible spectrophotometry using the 200
171 cm capillary cell. Figure 2 shows the decrease in non-aggregated AgNP concentration
172 observed in the seawater samples.
173 The Baltic fjord water had an enhanced DOC concentration of 277 ± 2.20 μM and a brackish
174 salinity of 17.19. The Spanish coastal seawater sample contained lower DOC (83.67 ± 0.75
175 μM) and a higher salinity of 34.65. Interactions between organic compounds and the AgNP

surface and its coating are likely to occur, producing small changes observed in the SPRB compared to high-purity water (Figure 2a,b).

Figure 2c shows a faster aggregation/oxidation kinetic (greater slope) of the low organic matter and high salinity Spanish coastal sample compared to the Baltic fjord seawater. Terrestrial fulvic/humic-like compounds found in the natural fjord waters, together with its low salinity, provide enhanced stabilization against aggregation (a detailed analysis is shown in the supplementary material). The SPRB shape and position values were comparable to the ones observed in the calibration. The SPRB showed only small changes during the experiments in seawater (Figure 2). The SPRB position and width at half height were ca. 415-421 nm and 65-70 nm (Baltic fjord), and 406-410 nm and 70-80 nm (Spanish coastal water). The SPRB changes observed between the different seawaters can be explained by differences in organic matter content. The changes in the refractive index of our solution media are expected to produce no significant variations (<1.4 nm) in the SPRB position (see supplementary material for details) [14].

The molar attenuation coefficient value used in the calculations can be influenced by the sample matrix, and size and coating of the NPs. The experiments were conducted in seawater, but we consider that the calculated molar attenuation coefficient is similar for the various matrices used, since no significant changes occurred in the SPRB position and shape.

The calculated AgNP concentration values in the Baltic fjord seawater were in good agreement with the initial AgNP concentration (20.4 ppb) used in the high-purity water experiments (Table 1). We obtained that concentration value before the start of the aggregation/oxidation process (<10 min) from SPRB height measurements. Nevertheless, the SPRB height detected at identical time in Spanish coastal seawaters was only 16.5 ppb (Table 1). This mismatch was observed only when the NP aggregation/oxidation occurred in the first seconds/minutes, and was likely due to fast reduction in SRPB as the quantity of non-

201 aggregated AgNPs decreased. As NPs aggregate and/or oxidize, the SPRB height will
202 decrease due to a reduction in the number of non-aggregated NPs. If the AgNPs interact to
203 form assemblies of different sizes, new resonance modes will appear [15]. Silver NP
204 aggregates may contribute to the SPRB signal yielding absorption at wavelengths higher than
205 500 nm. We separated this possible contribution from the signal of the non-aggregated NPs
206 by calculation of the height of the SPRB from a straight line traced from the base of the
207 SPRB between 325 and 500 nm [9].
208 The lowest SPRB height that was quantified (0.12 ± 0.02 A.U.) corresponded to an AgNP
209 concentration of 4 ppb in Spanish coastal seawater. Therefore, we showed here that a simple
210 and fast spectroscopy technique allows detection of non-aggregated AgNPs in seawaters at
211 low ppb levels, close to the projected future environmental concentrations.
212 In order to contribute to future improvements in the methodology presented here, the use of
213 complementary techniques, such as single particle ICP-MS, to verify the silver concentration
214 present in NPs and ionic forms in solution, will be important. This approach will allow us to
215 verify that the Ag present in solution during the calibration is mostly in NP form and
216 therefore contributes entirely to the SPRB.
217
218 **Conclusions**
219 This study demonstrates for the first time the quantification of AgNPs in environmental
220 samples at low ppb levels by UV-Visible spectrophotometry using capillary cells with an
221 optical path length up to 200 cm. The heights of the SPRB have been used to obtain a linear
222 calibration with an AgNP concentration range between 20-92 ppb. The molar attenuation
223 coefficient obtained from the calibration has been successfully used to calculate the AgNP
224 concentrations in natural seawater samples at low ppb levels.

225 **Supplementary material**. Details of experimental procedures and supplementary results.

226

227 **Figure captions**

228 **Figure 1**. Calibration for NM300K in aqueous solution at fixed pH 8.0±0.2. The height of the
229 SPRB was determined from UV-Visible spectra obtained using a capillary cell with an
230 optical path length of 100 cm.

231 **Figure 2**. a) Normalized spectra (Abs/Abs_0, Abs_0= Absorbance at t= 12 min) for NM300K
232 recorded at different times (black= 12, red= 22, green= 44, blue= 92 and grey= 197 min) in
233 Baltic fjord seawater. The magenta curve represents the normalized spectra in high-purity
234 water after 10 min.

235 b) Normalized spectra (Abs/Abs_0, Abs_0= Absorbance at t= 11 min) for NM300K recorded at
236 different times (black= 11, red= 22, green= 44, blue= 56 and grey= 71 min) in Spanish
237 coastal seawater. The magenta curve represents the normalized spectra in high-purity water
238 after 10 min.

239 c) Normalized SPRB height (SPRB height/ SPRB $height_{max}$) evolution over time for
240 NM300K AgNPs in Baltic fjord (black line) and Spanish (red line) seawaters. Spectra were
241 obtained using capillary cells with an optical path length of 200 cm.

242

243 **Acknowledgments**

244 King Abdulaziz University is acknowledged for their support. J. Pampín is acknowledged for
245 provision of the Matlab code used in this study.

246

247

248

249

250

251 **References**

252 [1] A. Bour, F. Mouchet, J. Silvestre, L. Gauthier, E. Pinelli, Environmentally relevant
253 approaches to assess nanoparticles ecotoxicity: A review, J Hazard Mater 283(0) (2015) 764-
254 777.

255 [2] A. Massarsky, V.L. Trudeau, T.W. Moon, Predicting the environmental impact of
256 nanosilver, Environ Toxicol Pharmacol 38(3) (2014) 861-873.

257 [3] F. Laborda, E. Bolea, G. Cepriá, M.T. Gómez, M.S. Jiménez, J. Pérez-Arantegui, J.R.
258 Castillo, Detection, characterization and quantification of inorganic engineered
259 nanomaterials: A review of techniques and methodological approaches for the analysis of
260 complex samples, Anal Chim Acta 904 (2016) 10-32.

261 [4] F. Laborda, J. Jimenez-Lamana, E. Bolea, J.R. Castillo, Selective identification,
262 characterization and determination of dissolved silver(I) and silver nanoparticles based on
263 single particle detection by inductively coupled plasma mass spectrometry, J Anal Atom
264 Spectrom 26(7) (2011) 1362-1371.

265 [5] S.M. Majedi, H.K. Lee, Recent advances in the separation and quantification of metallic
266 nanoparticles and ions in the environment, Trac Trend Anal Chem 75 (2016) 183-196.

267 [6] O. Geiss, C. Cascio, D. Gilliland, F. Franchini, J. Barrero-Moreno, Size and mass
268 determination of silver nanoparticles in an aqueous matrix using asymmetric flow field flow
269 fractionation coupled to inductively coupled plasma mass spectrometer and ultraviolet–
270 visible detectors, J Chromatogr A 1321(0) (2013) 100-108.

271 [7] F. Piccapietra, L. Sigg, R. Behra, Colloidal Stability of Carbonate-Coated Silver
272 Nanoparticles in Synthetic and Natural Freshwater, Environ Sci Technol 46(2) (2012) 818-
273 825.

[8] M. Baalousha, Y. Nur, I. Römer, M. Tejamaya, J.R. Lead, Effect of monovalent and divalent cations, anions and fulvic acid on aggregation of citrate-coated silver nanoparticles, Sci Total Environ 454–455(0) (2013) 119-131.

[9] P. Lodeiro, E.P. Achterberg, J. Pampín, A. Affatati, M.S. El-Shahawi, Silver nanoparticles coated with natural polysaccharides as models to study AgNP aggregation kinetics using UV-Visible spectrophotometry upon discharge in complex environments, Sci Total Environ 539 (2016) 7-16.

[10] L. Zhang, X. Li, R. He, L. Wu, L. Zhang, J. Zeng, Chloride-induced shape transformation of silver nanoparticles in a water environment, Environ Pollut 204 (2015) 145-151.

[11] D. Paramelle, A. Sadovoy, S. Gorelik, P. Free, J. Hobley, D.G. Fernig, A rapid method to estimate the concentration of citrate capped silver nanoparticles from UV-visible light spectra, Analyst 139(19) (2014) 4855-4861.

[12] J.R.G. Navarro, M.H.V. Werts, Resonant light scattering spectroscopy of gold, silver and gold-silver alloy nanoparticles and optical detection in microfluidic channels, Analyst 138(2) (2013) 583-592.

[13] M.E. Stewart, C.R. Anderton, L.B. Thompson, J. Maria, S.K. Gray, J.A. Rogers, R.G. Nuzzo, Nanostructured plasmonic sensors, Chem Rev 108(2) (2008) 494-521.

[14] A.D. McFarland, R.P. Van Duyne, Single Silver Nanoparticles as Real-Time Optical Sensors with Zeptomole Sensitivity, Nano Lett 3(8) (2003) 1057-1062.

[15] D.D. Evanoff, G. Chumanov, Synthesis and Optical Properties of Silver Nanoparticles and Arrays, ChemPhysChem 6(7) (2005) 1221-1231.

Funding: This research was supported by a Marie Curie Intra European Fellowship within the 7th European Community Framework Programme [grant agreement number PIEF-GA-2012-329575].

	High-purity water 100 cm	High-purity water 200 cm	Baltic fjord water 200 cm	Spanish coastal water 200 cm
SPRB height	0.23 ± 0.02	0.50 ± 0.02	0.51± 0.02	0.37 ± 0.01
[Ag] ppb	20 ± 2	23 ± 2	24 ± 2	16.5 ± 0.9

GRAPHICAL ABSTRACT

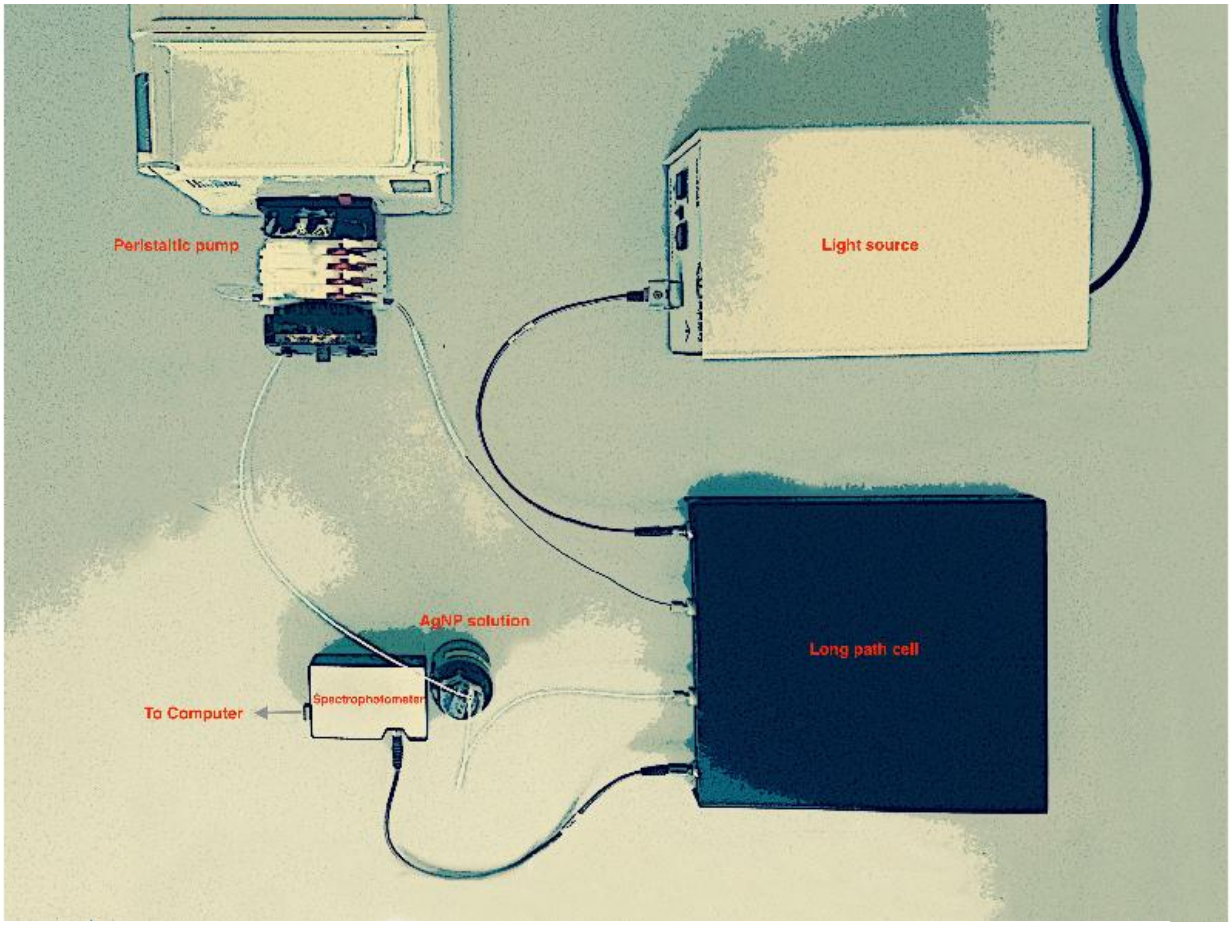
Peristaltic pump
Light source
AgNP solution
Long path cell
Spectrophotometer
To Computer

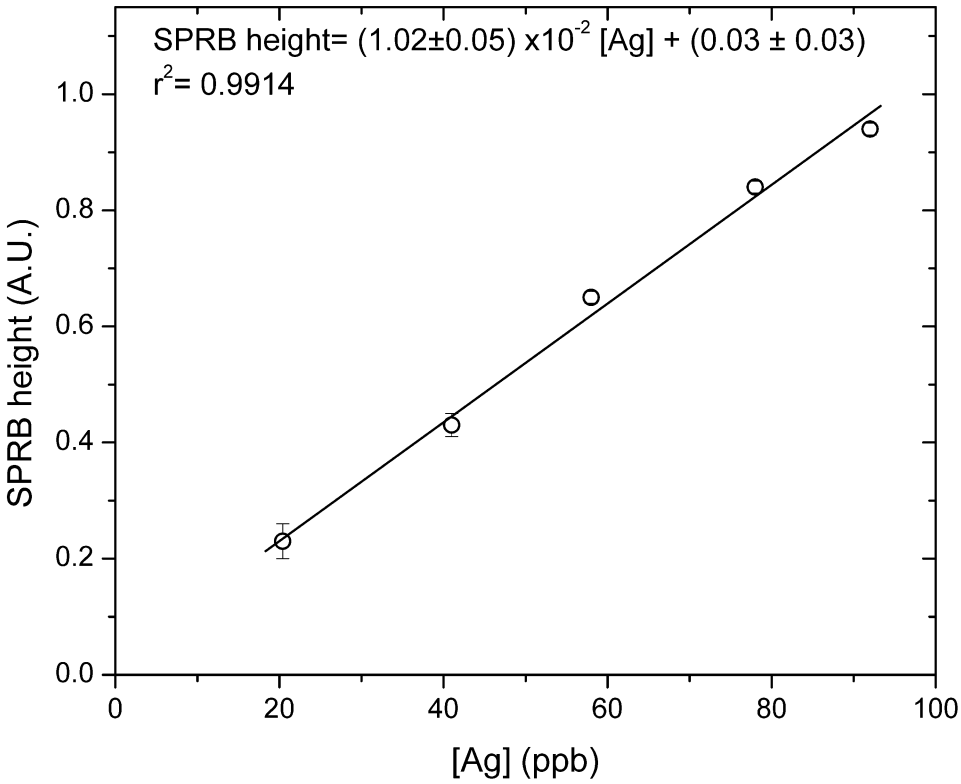
SPRB height= (1.02±0.05) x10^{-2} [Ag] + (0.03 ± 0.03)
r^2= 0.9914
SPRB height (A.U.)
[Ag] (ppb)
0.0
0.2
0.4
0.6
0.8
1.0
0
20
40
60
80
100

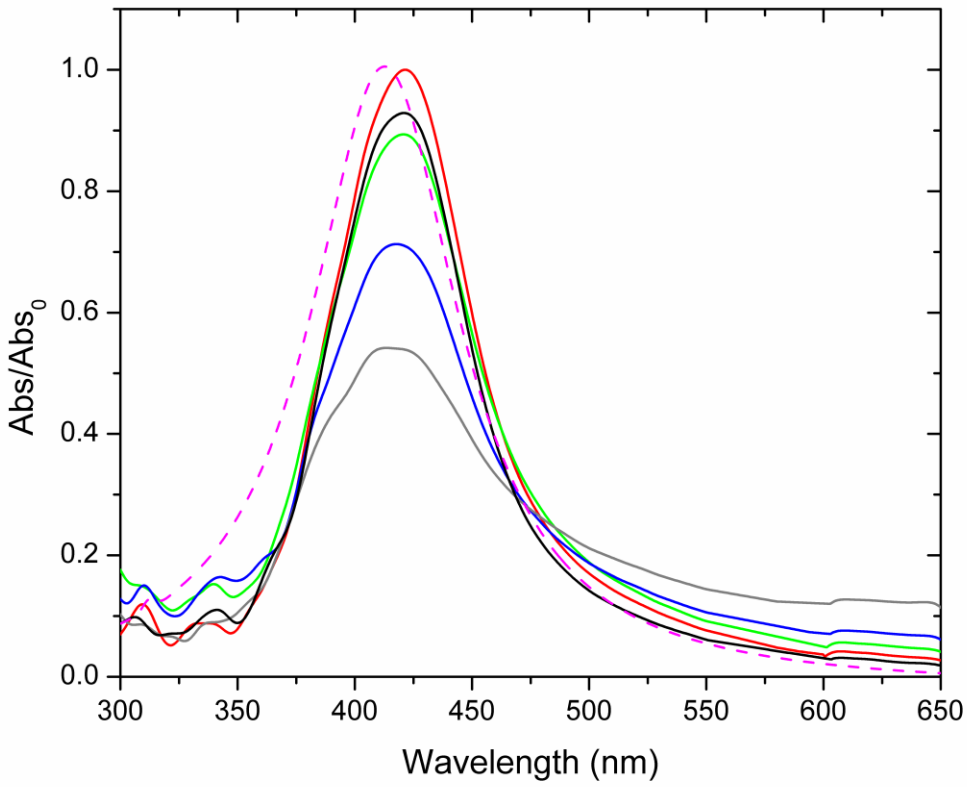
1.0
0.8
0.6
0.4
0.2
0.0
Abs/Abs0
300
350
400
450
500
550
600
650
Wavelength (nm)

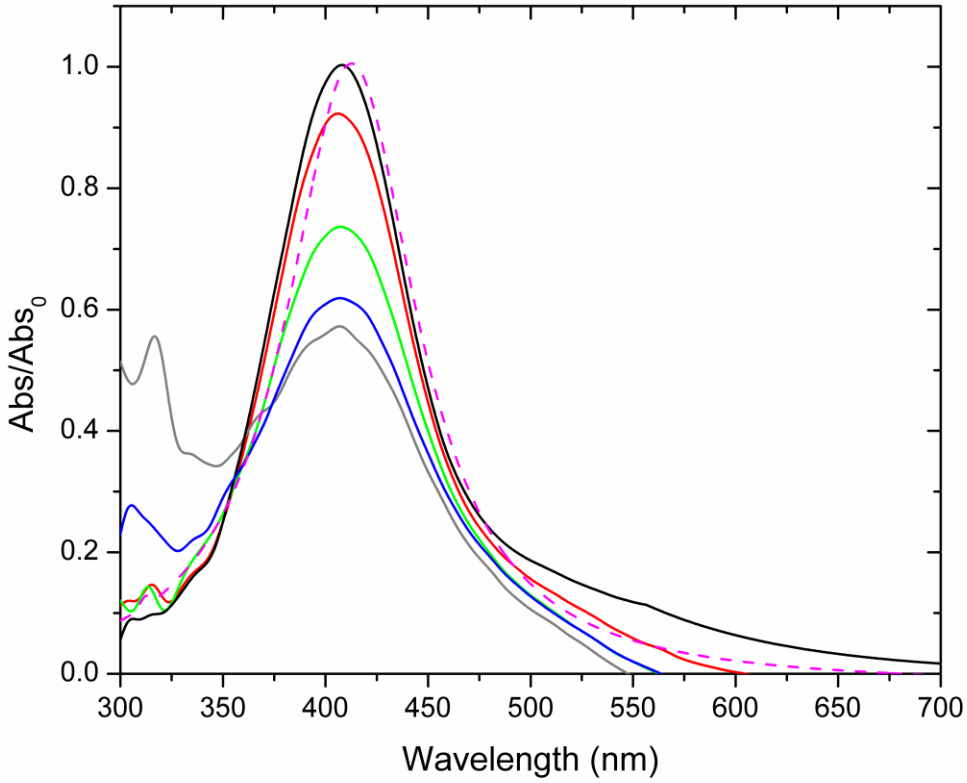
1.0
0.8
0.6
0.4
0.2
0.0
Abs/Abs0
300
350
400
450
500
550
600
650
700
Wavelength (nm)

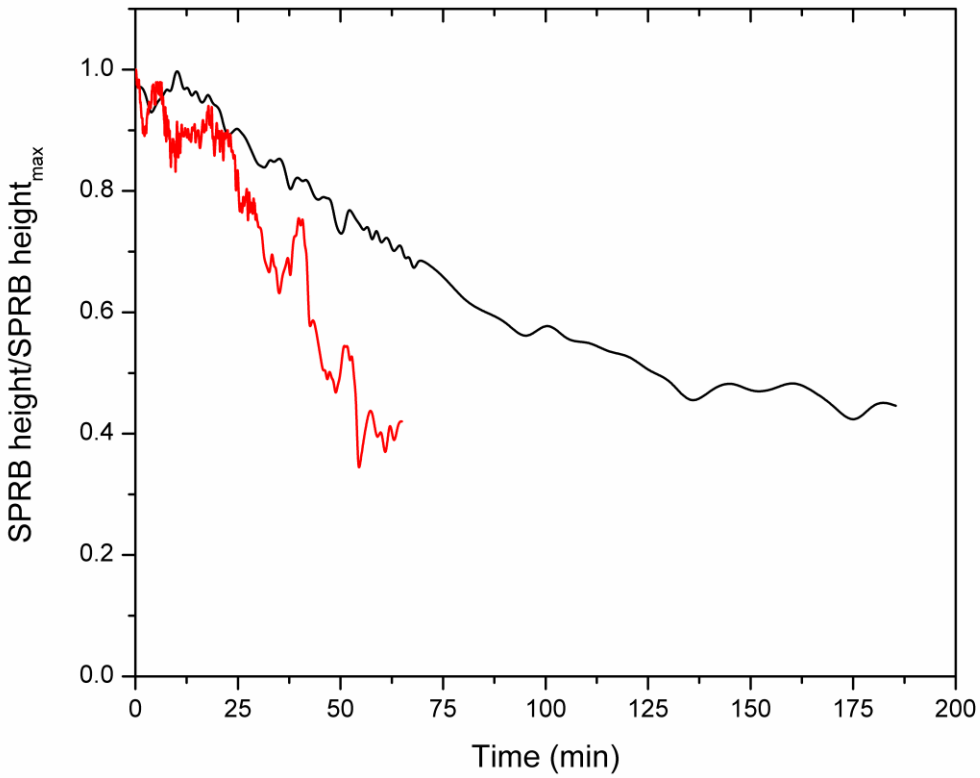

Highlights

- Detection and quantification of AgNP at ppb levels in natural seawater samples
- The use of long path cells (up to 200 cm) in UV-Visible spectrophotometry is proposed
- Knowledge of the molar attenuation coefficient of the NP under study in the sample matrix is required